Research Article

BIOMEDICAL Journal of Scientific & Technical Research

ISSN: 2574 -1241

DOI: 10.26717/BJSTR.2023.48.007646

Numerical Analysis of the Micro-Rotational Effects on Nanofluid Flow with Chemical Reaction Effects

Khuram Rafique[1*], Adeel Khalid[2], Nida Ibrar[3], Ayesha Ijaz[2] and Ayesha Munir[1]

[1]*Depaertment of Mathematics, University of Sialkot, Pakistan*

[2]*Department of Zoology, University of Sialkot, Pakistan*

[3]*Department of Mathematics, University of Sargodha, Pakistan*

***Corresponding author:** Khuram Rafique, Department of Mathematics, University of Sialkot, 51040, Sialkot, Pakistan

ARTICLE INFO

Received: January 20, 2023

Published: February 06, 2023

Citation: Khuram Rafique, Adeel Khalid, Nida Ibrar, Ayesha Ijaz and Ayesha Munir. Numerical Analysis of the Micro-Rotational Effects on Nanofluid Flow with Chemical Reaction Effects. Biomed J Sci & Tech Res 48(3)-2023. BJSTR. MS.ID.007646.

ABSTRACT

Nanotechnology and nanoscience and their wide uses in the biomedical due to the unique and novel properties of nanoparticles have become a spread field for research worldwide. The properties of nanoparticles based on the shape, size and the components. These days' different nanoparticles are under investigation for their utilization in the biomedical science especially for the cancer therapeutics. This paper is prepared for the investigation of numerical simulation of nanoparticles affected by the micro-rotation by incorporating the chemical reaction impacts. Moreover, the convective boundary conditions are considered. First we convert the PDE's into ODE's by utilizing the suiss transformations. Further numerical technique applied for the graphs and numerical values of the energy and mass transportation. We recovered that the power index factor and magnetic effect increment diminishes the velocity distribution. The convective parameter increases the temperature distribution of the nanoliquid.

Keywords: Micropolar Nanofluid; MHD; Convective Boundaries; Chemical Reaction; Heat Generation or Absorption; Inclined Surface

Introduction

The utilization of nanotechnology permits producing materials that have size under 100 nm. These nanomaterials dependent on their structure and qualities can be portioned into four classifications: metal-based nanomaterials, carbon-based nanomaterials, composite and dendrimers. Choi, et al. [1] first assessed the phrasing nanofluid. Liquids that possess particles estimates not exactly 100 nm can be named as nanofluid. The classes of various nanoparticles are characterized by particle material, size, base liquid and concentration relating to the nanofluid. These nanoparticles could be suspended into any regular liquid, for example, water, oil, ethylene glycol to frame nanofluids. Nanoparticles offer better improvement regarding thermo-physical properties over micro scale particles. The utilization of nanofluids ranges from improving efficiency of diesel generator to air molding cooling, control plant cooling, car, and so forth. Ordinarily as heat exchange base liquids, water and ethylene glycol are utilized. Nanoparticles are delivered by utilizing different substances, which are commonly divided into metal-oxide (for example $Cu0, Al_20_3$), metallic (for example copper, aluminum) and various particles (for example carbon nanotubes) [2]. Nanofluid flow over a slanted sheet by considering the magnetic effects calculated by Suriyakumar, et al. [3]. Khan, et al. [4] scrutinized the Jeffery nanofluid flow through a slanted sheet. Thumma, et al. [5] studied the nanofluid flow over a nonlinear inclined extending sheet. Recently, many researchers argued on the nanofluid flow by incorporating changed effects [6-10]. The impact of chemical reaction has attained significant attention of recent researcher because of its vital role in food processing and chemical engineering. Bohra [11] studied the slanted sheet with the incorporation of chemical species. Further chemical reaction has been taken for the analysis of nanoliquid flow through an inclined sheet is discussed by Bhuvaneswari, et al. [12]. Sandeep, et al. [13] considered the chemical reaction in their study for the nanoliquid.

Moreover, hydrodynamic flow for a stretchy surface was discussed by Shit, et al. [14]. For further detailed about flow of different geometries with chemical reaction see [15-20]. The ongoing advancement in non-Newtonian fluids flows upraise in numerous various parts of applied sciences, geophysics and engineering. Because of this non-Newtonian fluid have gotten significance intrigue, one such fluid is micropolar fluid. This fluid is described by shear-stress-strain relationship, which generously deviates from classical Newtonian liquids for example Navier-Stokes equation. Such fluids abound in

compound industrial developments for example, in petrochemical constituents processing and slurry. Eringen [21] presented the idea about micropolar liquids on the basis of constituent's equations. Rafique, et al. [22] studied micro-rotational impacts on the nanliquid flow numerically. Further, Rafique, et al. [23] examined the micropolar nanoliquid flow on a slanted surface by numerical technique and presents the magnetic factor impacts on the velocity profile. Abbas, et al. [24] discussed the flow of microplar liquid on an exponential stretchy sheet by incorporating the slip impacts. For more studies relevant to the micropolar liquid see the references [25-28]. In any article, up until today, no effort has been made to scrutinize the double diffusive effects on affected micropolar nanofluid flow on power law stretchy sheet with convective boundaries. Thus, the main goal of the current problem is to investigate the conjugate effects on the flow of micropolar nanofluid on the inclined stretching sheet with chemical reaction and heat generation. The numerical outcomes from the converted ordinary differential equations have been elucidate via Keller box analysis because it is more efficient as compared to other methods.

Problem Formulation

The incompressible nanoliquid affected by the micro-rotation has been considered in this analysis. The nanoliquid flow on the slanted surface and chemical reaction effects with convective boundaries are incorporated for the investigation. Flow is produced due to the nonlinear stretching slanted surface. The inclination γ of the stretchy surface makes with the vertical direction. Convective boundary conditions for heat exchange are considered. Further the impacts of chemical reaction and heat generation or absorption has been examined numerically. In view of the assumptions and the reference [29] the flow equations are given as for the current investigation.

$$\frac{\partial u}{\partial x}+\frac{\partial v}{\partial y}=0 \quad (1)$$

$$u\frac{\partial u}{\partial x}+v\frac{\partial u}{\partial y}=\left(\frac{\mu+k_1^*}{\rho}\right)\frac{\partial^2 u}{\partial y^2}+\left(\frac{k_1^*}{\rho}\right)\frac{\partial N^*}{\partial y}+g\left[\beta_t\left(T-T_\infty\right)-\beta_c\left(C-C_\infty\right)\right]\cos y-\left(\frac{\sigma B_0^2(x)}{\rho}\right)u$$

$$u\frac{\partial N^*}{\partial x}+v\frac{\partial N^*}{\partial y}=\left(\frac{y^*}{j^*\rho}\right)\frac{\partial^2 N^*}{\partial y^2}-\left(\frac{K_1^*}{j^*\rho}\right)\left(2N^*+\frac{\partial u}{\partial y}\right) \quad (3)$$

$$u\frac{\partial T}{\partial x}+v\frac{\partial T}{\partial y}=\alpha\frac{\partial^2 T}{\partial y^2}+\tau\left[D_B\frac{\partial c}{\partial y}\frac{\partial T}{\partial y}+\frac{D_T}{T_\infty}\left(\frac{\partial T}{\partial y}\right)^2\right]+\frac{Q_0}{\rho c_p}\left(T-T_\infty\right) \quad (4)$$

$$u\frac{\partial c}{\partial x}+v\frac{\partial c}{\partial y}=D_B\frac{\partial^2 c}{\partial y^2}+\frac{D_T}{T_\infty}\frac{\partial^2 T}{\partial y}+R^*\left(C-C_\infty\right) \quad (5)$$

Where u and v are the components of velocity in x and y directions, respectively, g is the acceleration due to gravity, B_0 is the uniform magnetic field strength, σ denotes the electrical conductivity, μ is the viscosity, ρf is the density of the base fluid, ρ_p denotes the density of the nanoparticle, k_1^* is the vortex viscosity, β_t is the coefficient of thermal expansion, β_c denote the coefficient of concentration expansion, γ^* is the spin gradient viscosity, j^* is the micro inertia per unit mass, N^* is the micro-rotation or angular velocity, D_B denote the Brownian diffusion coefficient and D_T denotes the thermophoresis diffusion coefficient, k is the thermal conductivity. The subjected boundary conditions are.

$$u=u_w(x)=ax^m, v=V_w, -k\frac{\partial T}{\partial y}=h_f\left(T_f-T\right), N^*=-m_0\frac{\partial u}{\partial y}, C=C_w \text{ at } y=0,$$
$$u\to u_\infty(x)=0, v\to 0, T\to T_\infty, N^*\to 0, C\to C_\infty \text{ at } y\to\infty, \quad (6)$$

The nonlinear partial differential equations are reduced into nonlinear ordinary differential equations. For that purpose, the stream function $\psi=\psi(x,y)$ is defined as

$$u=\frac{\partial\psi}{\partial y}, v=-\frac{\partial\psi}{\partial x}, \quad (7)$$

Where continuity equation in equation (1) is satisfied identically. The similarity transformations are defined as

$$\psi=\sqrt{\frac{2vax^{m+1}}{m+1}}f(\eta), \theta(\eta)=\frac{T-T_\infty}{T_w-T_\infty},$$
$$\phi(\eta)=\frac{C-C_\infty}{C-C_\infty}, \eta=y\sqrt{\frac{(m+1)ax^{m-1}}{2v}}.$$
$$N^*=ax^m\sqrt{\frac{a(m+1)x^{m-1}}{2v}}g(x), \quad u=x^m f'(\eta), \quad (8)$$
$$Where \quad V=-\sqrt{\frac{av(m+1)x^{m-1}}{2}}\left[f(\eta)+\frac{m+1}{m-1}\eta f'(\eta)\right],$$

The equations (2) to (5) have been converted with the utilization of equation (8) into

$$(1+K)f'''+ff''-\left(\frac{2m}{m+1}\right)f'^2+Kh'+\frac{2}{m+1}(\lambda\theta+\delta\phi)\cos y-\frac{2}{m+1}Mf'=0, \quad (9)$$

$$\left(1+\frac{K}{2}\right)h''+fh'\frac{3m-1}{m+1}f'h-\frac{2K}{m+1}\left(2h+f''\right)=0 \quad (10)$$

$$\left(\frac{1}{pr}\right)\theta'' + f\theta' + \lambda_1\theta' + Nb\phi'\theta' + Nt\theta'^2 = 0 \quad (11)$$

$$\phi'' + Lef\phi' + Nt_b\theta'' - LeR\phi = 0 \quad (12)$$

Where

$$M = \frac{\sigma B_0^2}{a\rho}, Le = \frac{v}{D_B}, \Pr = \frac{v}{\alpha}, N_b = \frac{\tau D_B (C_w - C_\infty)}{v}, N_t = \frac{\tau D_t (T_w - T_\infty)}{vT_\infty}, K = \frac{k_1^*}{\mu},$$
$$Gr_x = \frac{g\beta_t (T_w - T_\infty)x^{-1}}{av}, R\mathrm{e}_x = \frac{u_w(x)x}{v}, Gc_x = \frac{g\beta_c (C_w - C_\infty)x^{-1}}{av}, Nt_b = \frac{N_t}{N_b}, \lambda_1 = \frac{Q_0}{a\rho c_p}, R = \frac{R^*}{a},$$

(13)

Here, primes means the differentiation concerning η , λ Buoyancy parameter, δ Solutal buoyancy parameter, M is the magnetic parameter called Hartmann number, v is the kinematic viscidness of the liquid, p_r denotes the Prandtl number, Le denotes the Lewis number, K is the dimensionless vertex thickness, λ_1 use for heat generation or absorption, R use for chemical reaction factor.

In view of [30], $\lambda = \frac{gn(T_w - T_\infty)}{av} and \delta = \frac{gn_1(T_w - T_\infty)}{av}$, $where, n = x^{-1}\beta_t and n_1 = x^{-1}\beta_c.$

The corresponding boundary conditions are transformed to

$$f(n) = s,\ f'(n) = 1,\ \theta'(0) = -\gamma_1\sqrt{2/(m+1)}\left(1-\theta(0)\right),\ \phi(\eta) = 1 at \eta = 0$$
$$f'(n) \to 0, h(\eta) \to 0,\ \phi(\eta) \to 0 as\ \eta \to \infty$$

(14)

Here, γ_1 denotes the Biot number which is convective factor.

The quantities of engineering interest are

$$Nu_x = \frac{xq_w}{k(T_w - T_\infty)}, (Nusselt\ number)\ Sh_x = \frac{xq_m}{D_B(C_w - C_\infty)}, (Sherwood\ number)\ Cf = \frac{t_w}{u_w^2\rho f}, (Skin\ friction)$$

The related relations for the reduced Nusselt number $-\theta(0)$, the reduced Sherwood number $-\phi(0)$, and skin-friction coefficient, are denoted as

$$C_{fx}(0) = \frac{C_f}{2}\sqrt{\frac{2}{m+1}R\mathrm{e}_x} - \theta'(0) = \frac{Nu}{\sqrt{\mathrm{Re}_x(m+1)/2}}, \phi'(0) = \frac{Sh}{\sqrt{\mathrm{Re}_x(m+1)/2}},$$

(15)

Where, $\mathrm{Re}_x = u_w(x)x/\nu$ is the local Reynolds number.

Results and Discussion

This section of study explains the numerical outcomes of physical parameters of our concern containing Brownian motion factor Nb , thermophoresis assumed by Nt , magnetic factor M , buoyancy factor λ , solutal buoyancy constraint δ , inclination factor γ , Prandtl number p_r , Lewis number Le , chemical reaction R , heat generation or absorption parameter λ_1 , Biot number γ_1 , material factor K and parameter m numerous statistics and tables are arranged. The current results matched with the outcomes of Khan and Pop [31] in Table 1 The effects on $-\theta'(0), -\phi'(0)$ and $C_{fx}(0)$ for various factors $Nb, \beta, Nt, M, N, \lambda, \delta, \gamma, P_r, Le, \gamma_1$ and m are exposed in Table 2. From Table 2, it is observed that the reduced Nusselt number drops by improving the Brownian motion effect and the opposite relation seen in the case of Sherwood number .Moreover, the magnitudes of reduced Nusselt number and Sherwood number are reduce on enhancing the thermophoresis impacts. Physically, these trends are acceptable because on enhancing the Brownian motion parameter, a large extent of fluid affected and consequently thickening the boundary layer (Table 3). On the other hand, Nusselt and Sherwood number decline against the large values of Biot number γ_1 . Besides, skin friction shows directly proportional relation with the magnetic effect and nonlinear stretching parameter. It can observed that the buoyancy and solutal buoyancy parameters upsurge the Sherwood and Nusselt number for the higher values and decline the skin friction.

Velocity Profile

Figure 1 reveals that the velocity field shows an inverse relation with the magnetic factor. The reason behind this is the enhancement in the magnetic parameter produces the drag force on the sheet, which declines the velocity of the fluid. Similar effect presents in the case of angular velocity against magnetic parameter in the Figure 2. On the other hand, the similar result presents the Figure 3 again large magnitude of magnetic effect. Physically, the viscosity of the boundary layer reduces on increasing the magnetic factor. Figure 4 represents an opposite result against the nonlinear stretching parameter values. The enhancement in the nonlinear stretching factor causes the reduction in the momentum boundary layer thickness. Besides, in Figure 5 the velocity profile enhances against the large impact of parameter . In addition, the velocity field slows down on increasing the inclination parameter drawn in Figure 6. Moreover, the circumstances point out that in the case of the maximum gravitational force apply on flow because in this state the sheet will be vertical. On the other hand, the sheet will be horizontalin the case of $\gamma = 90^o$ due to which the power of the bouncy forces drops which causes the decline in velocity profile.

Table 1: Contrast of $-\theta'(0)$ and $-\phi'(0)$ against $\gamma = 90^o, \gamma_1 \to \infty, M, K, , m, \delta, \lambda, R, , \lambda_1 = 0$ with $P\mathrm{r} = Le$.

Nb	Nt	Khan and Pop [29]		Present Results	
		$-\phi'(0)$	$-\theta'(0)$	$-\phi'(0)$	$-\theta'(0)$
0.1	0.1	2.1294	0.9524	2.1294	0.9524
0.2	0.2	2.5152	0.3654	2.5152	0.3654
0.3	0.3	2.6088	0.1355	2.6088	0.1355
0.4	0.4	2.6038	0.0495	2.6038	0.0495
0.5	0.5	2.5731	0.0179	2.5731	0.0179

Table 2. Values of $-\theta(0), -\phi(0)$ and $C_{fx}(0)$.

Nb	Nt	Pr	Le	M	K	$\gamma 1$	R	$\lambda 1$	λ	δ	S	m	γ	$-\theta(0)$	$-\phi(0)$	$C_{fx}(0)$
0.1	0.1	7.0	5.0	0.1	1.0	0.1	1.0	0.1	0.1	0.9	0.1	0.5	450	0.0905	1.0003	0.9205
0.3	0.1	7.0	5.0	0.1	1.0	0.1	1.0	0.1	0.1	0.9	0.1	0.5	450	0.0364	1.0357	0.9283
0.1	0.3	7.0	5.0	0.1	1.0	0.1	1.0	0.1	0.1	0.9	0.1	0.5	450	0.0864	0.9457	0.8983
0.1	0.1	10.0	5.0	0.1	1.0	0.1	1.0	0.1	0.1	0.9	0.1	0.5	450	0.0930	1.0015	0.9199
0.1	0.1	7.0	10.0	0.1	1.0	0.1	1.0	0.1	0.1	0.9	0.1	0.5	450	0.0802	1.5694	1.0085
0.1	0.1	7.0	5.0	0.5	1.0	0.1	1.0	0.1	0.1	0.9	0.1	0.5	450	0.0876	0.9437	1.2569
0.1	0.1	7.0	5.0	0.1	5.0	0.1	1.0	0.1	0.1	0.9	0.1	0.5	450	0.0940	1.0687	1.6334
0.1	0.1	7.0	5.0	0.1	1.0	0.2	1.0	0.1	0.1	0.9	0.1	0.5	450	0.1680	0.9742	0.9076
0.1	0.1	7.0	5.0	0.1	1.0	0.1	3.0	0.1	0.1	0.9	0.1	0.5	450	0.1021	0.0849	0.8293
0.1	0.1	7.0	5.0	0.1	1.0	0.1	1.0	0.3	0.1	0.9	0.1	0.5	450	0.0510	1.0328	0.9214
0.1	0.1	7.0	5.0	0.1	1.0	0.1	1.0	0.1	1.0	0.9	0.1	0.5	450	0.0906	1.0030	0.8929
0.1	0.1	7.0	5.0	0.1	1.0	0.1	1.0	0.1	0.1	2.0	0.1	0.5	450	0.0929	1.0417	0.5166
0.1	0.1	7.0	5.0	0.1	1.0	0.1	1.0	0.1	0.1	0.9	0.3	0.5	450	0.0417	0.4995	0.7215
0.1	0.1	7.0	5.0	0.1	1.0	0.1	1.0	1.0	1.0	1.0	0.0	0.5	450	0.1207	1.2975	0.9767
0.1	0.1	7.0	5.0	0.1	1.0	0.1	1.0	1.0	1.0	1.0	-0.3	0.5	450	0.2272	2.3060	1.2197
0.1	0.1	7.0	5.0	0.1	1.0	0.1	1.0	1.0	1.0	1.0	0.1	1.5	450	0.0883	0.9598	1.2546
0.1	0.1	7.0	5.0	0.1	1.0	0.1	1.0	1.0	1.0	1.0	0.1	0.5	900	0.0900	0.9919	0.9951

 DOI: 10.26717/BJSTR.2023.48.007646

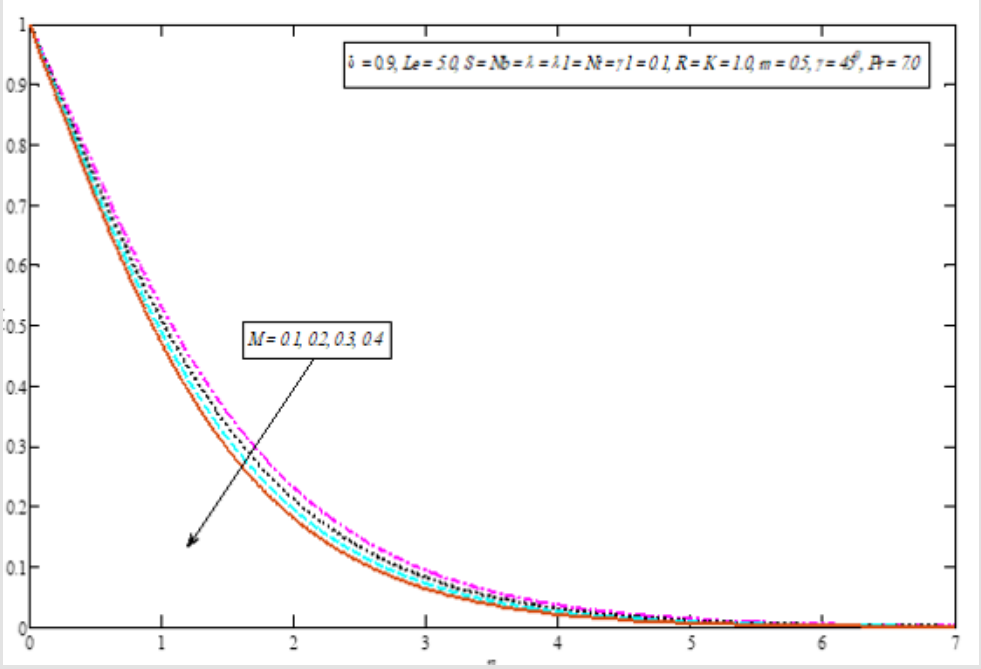

Figure 1: Velocity profile against M .

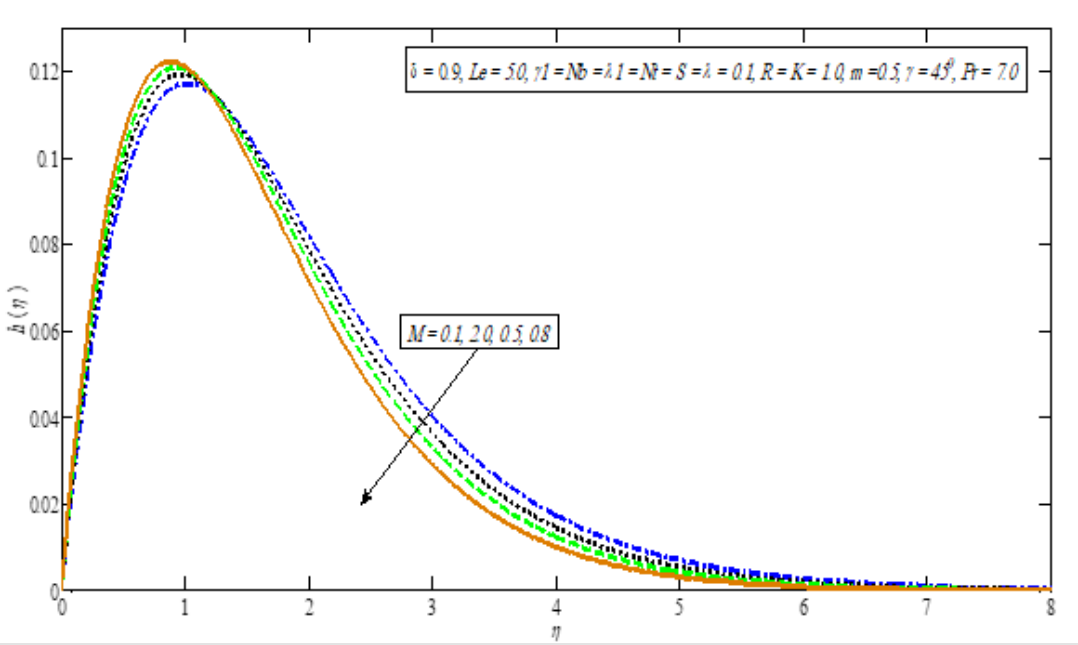

Figure 2: Angular velocity profile against M .

 DOI: 10.26717/BJSTR.2023.48.007646

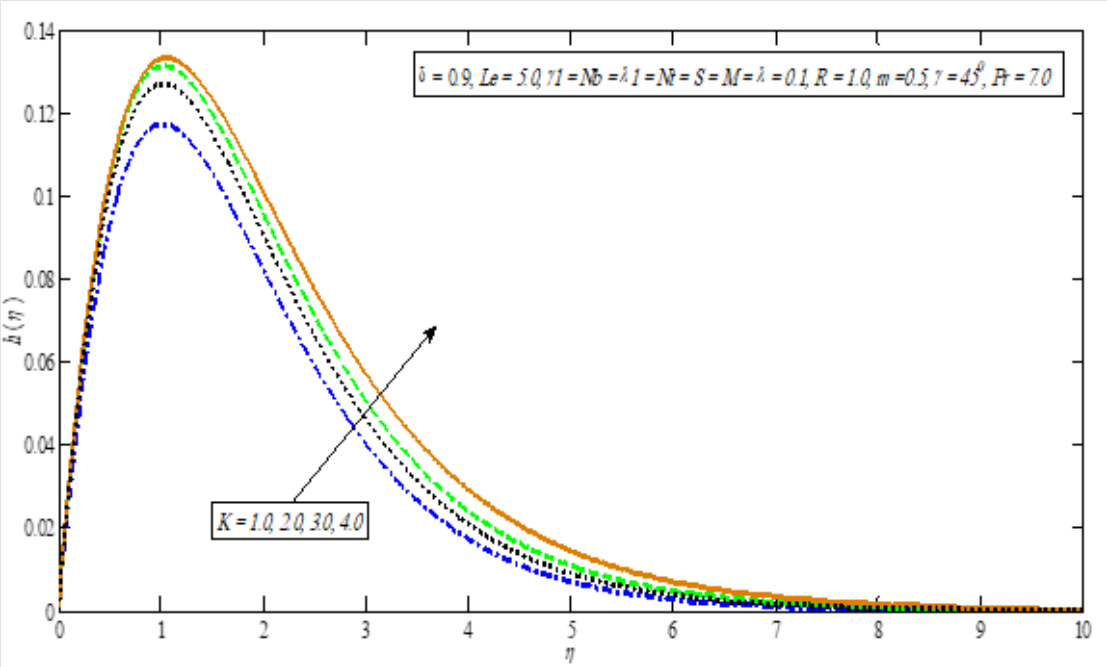

Figure 3: Angular velocity profile against K .

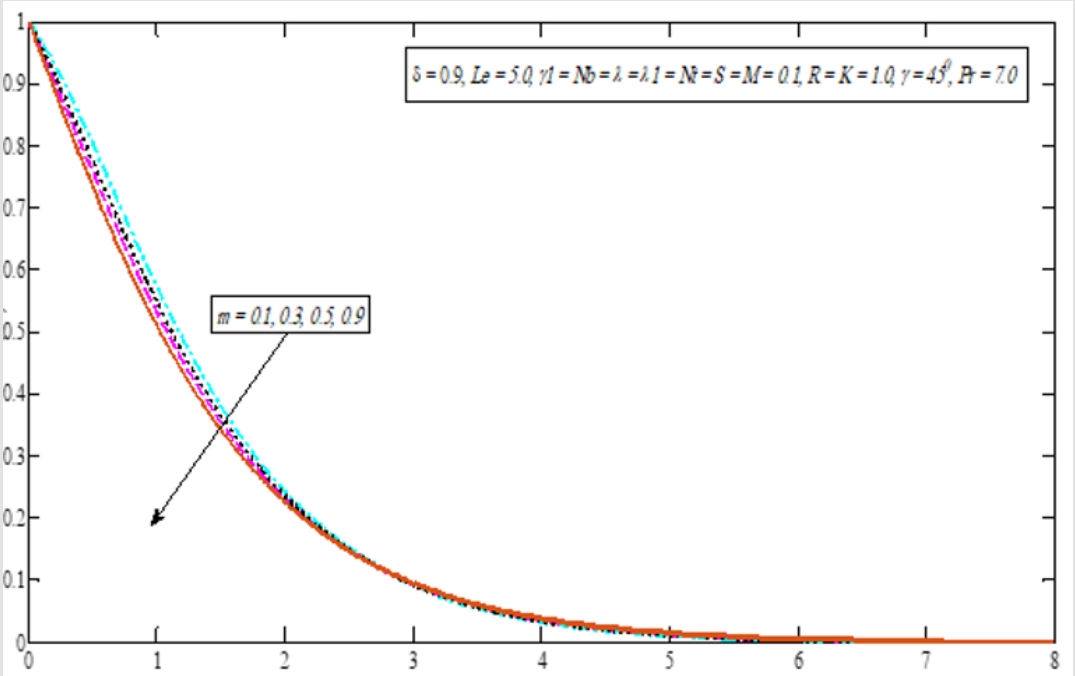

Figure 4: Velocity profile against M .

 DOI: 10.26717/BJSTR.2023.48.007646

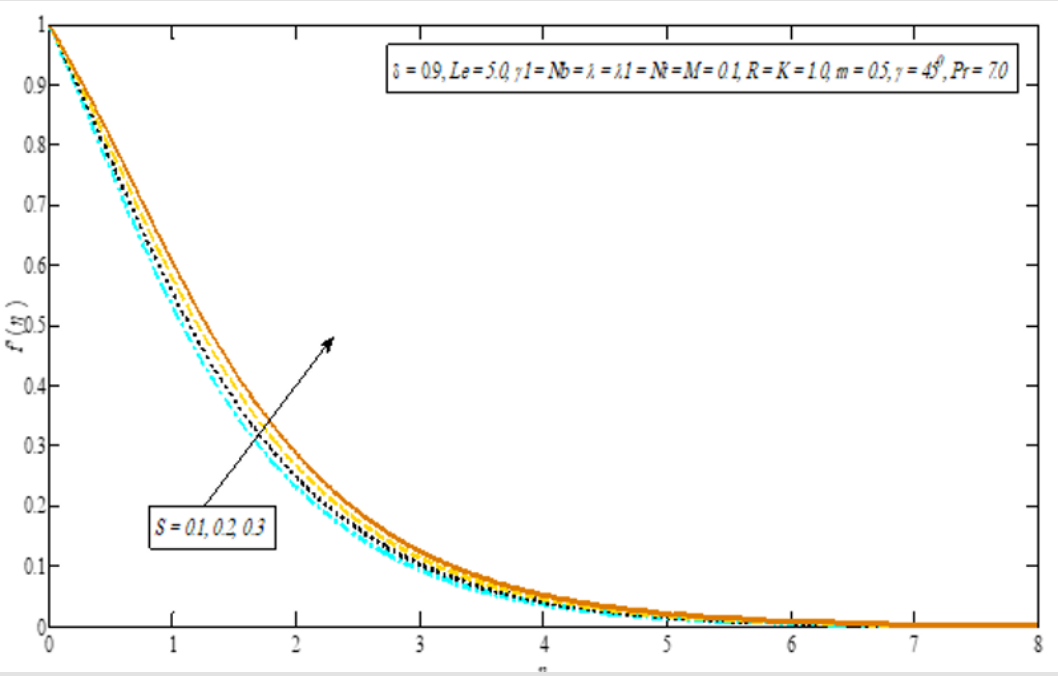

Figure 5: Velocity profile against S.

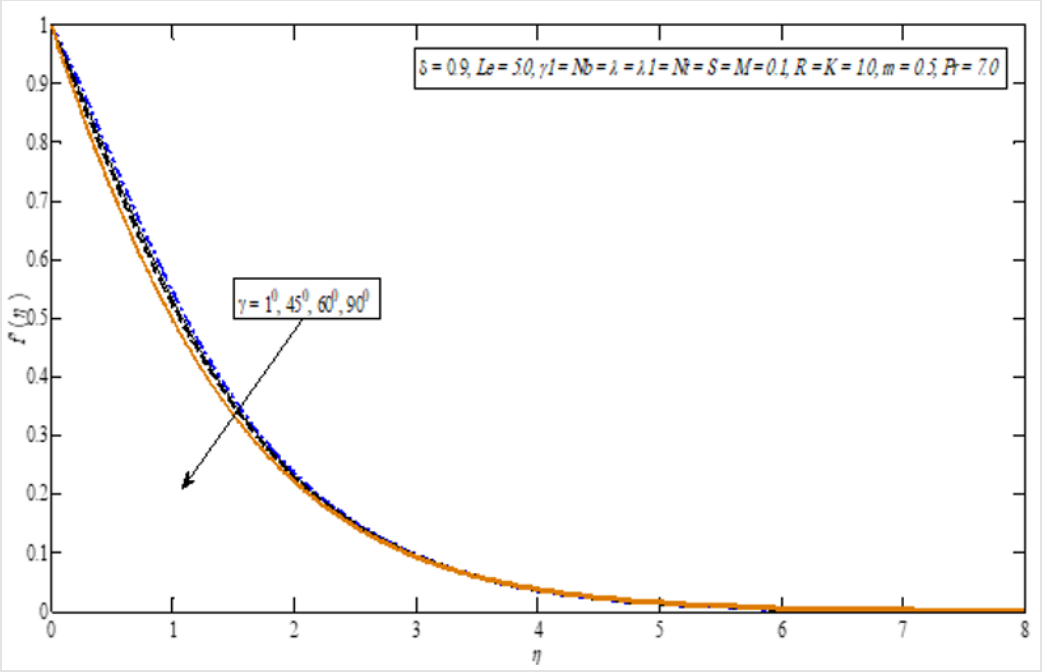

Figure 6: Velocity profile against γ.

Temperature Profile

Behavior of temperature profile against Biot number presented in Figure 7. Clearly the boundary layer thickness increases as a result temperature profile rises. For large values of Biot number heat exchange coefficient increases. It is observed that if $\gamma_1 \to \infty$ relates to the constant wall temperature. The temperature profile relates directly proportional to the Brownian motion effect shown in Figure 8. It is due to the fact that the Brownian motion parameter enhances

the boundary layer heat which leads to increase the fluid temperature. The change between reference temperature and wall temperature improved by rising the thermophoresis impacts due to which temperature profile increases (see Figure 9). The heat generation increases the velocity of the liquid directly, which leads to generate the heat in the flow region and the temperature increase with in the thermal boundary layer shown in Figure 10. The temperature profile increases by improving Prandtl number shown in Figure 11. As steadily rises, this corresponds to the thinner thermal boundary layer and weaker thermal diffusivity. It is important to reference here bigger values of Pr represent the high viscosity liquids such as oils. On the other hand, lower values Pr denote the liquid like materials which have low viscosity and high thermal conductivity.

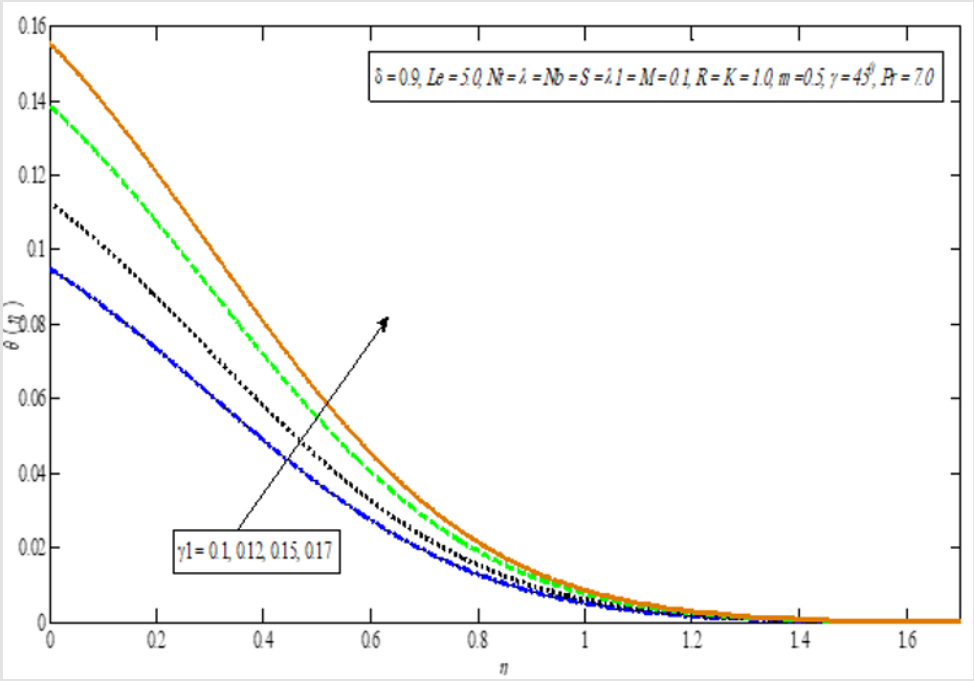

Figure 7: Temperature profile against γ_1.

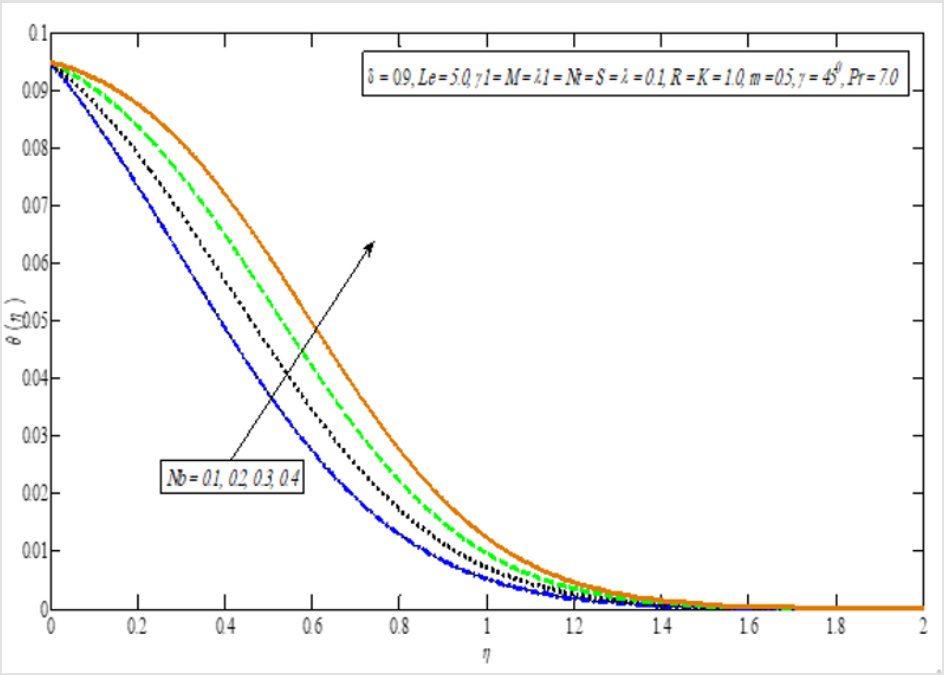

Figure 8: Temperature profile against Nb.

DOI: 10.26717/BJSTR.2023.48.007646

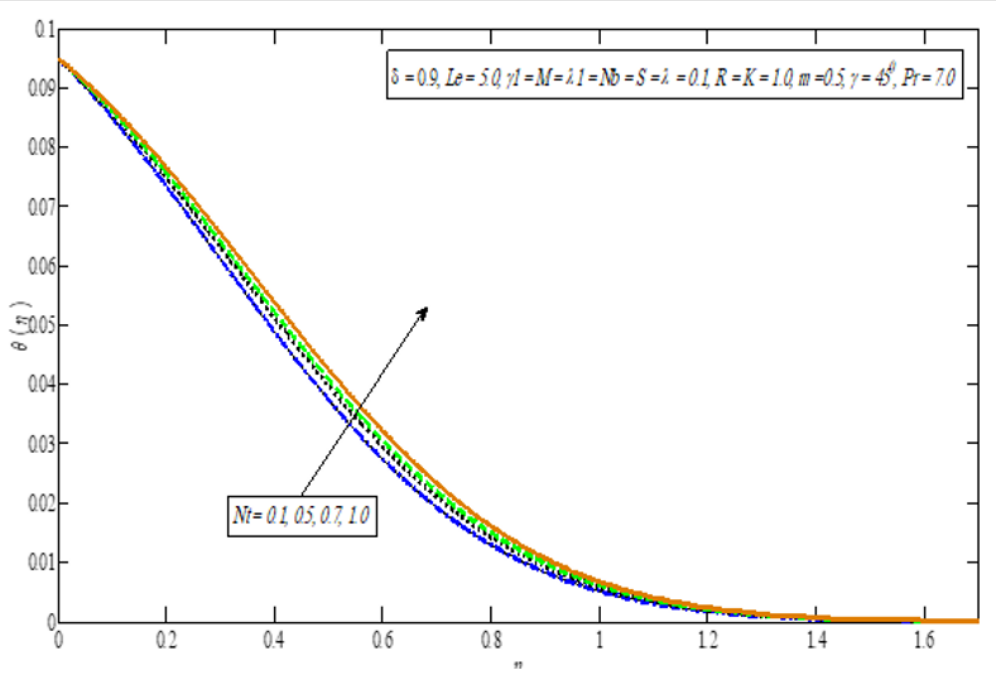

Figure 9: Temperature profile against Nt.

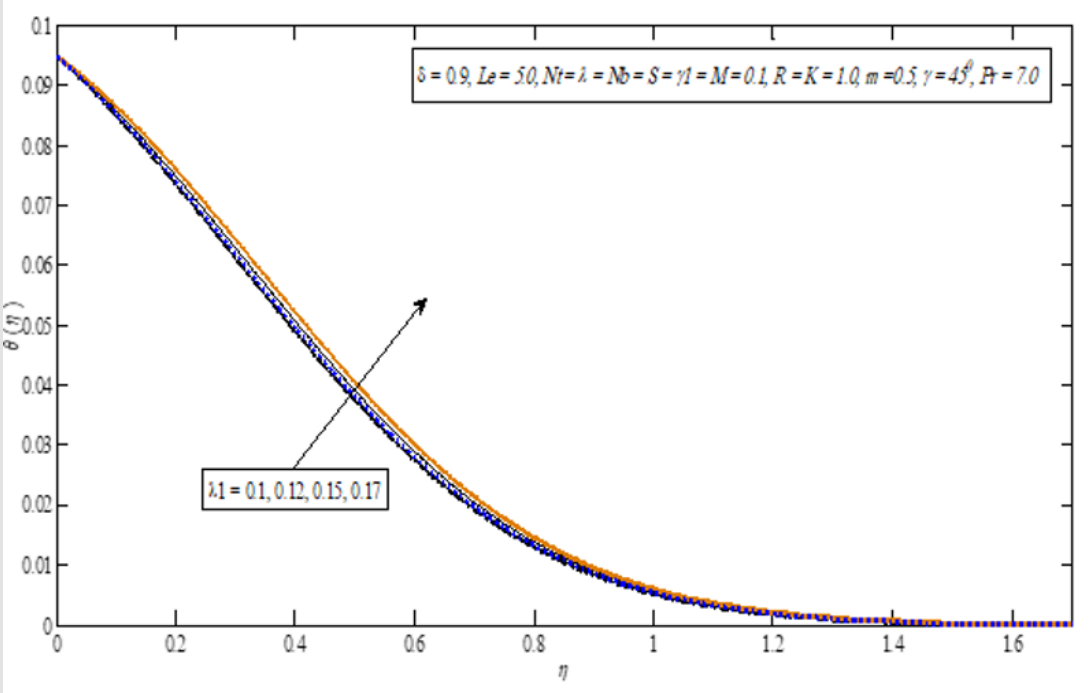

Figure 10: Temperature profile against λ_1.

 DOI: 10.26717/BJSTR.2023.48.007646

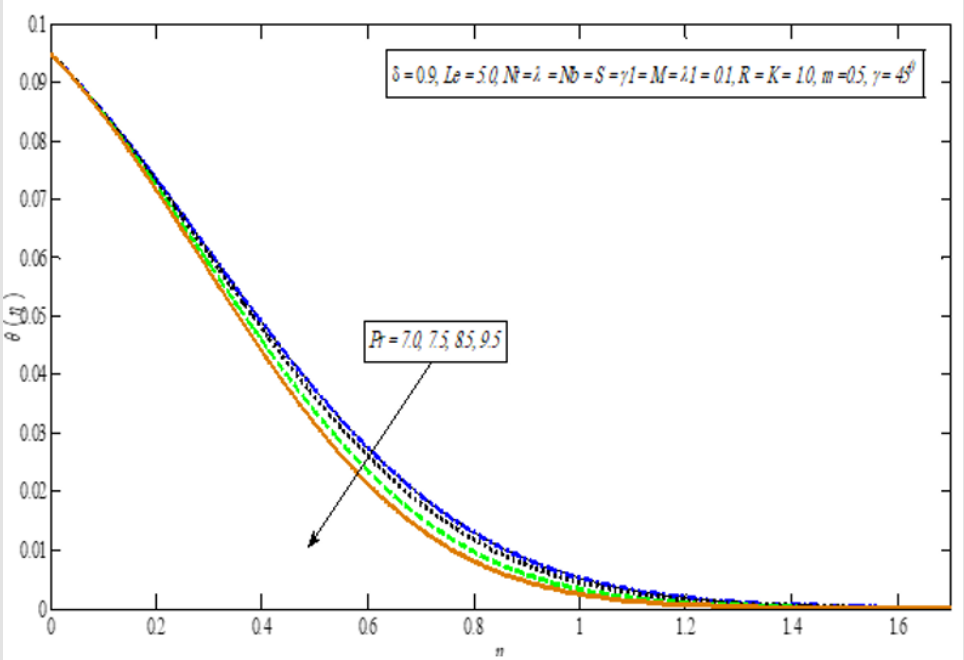

Figure 11: Temperature profile against Pr.

Concentration Profile

An opposite result has seen in the case of concentration profile as compared to temperature profile against different values Brownian motion impacts (see Figure 12). The concentration at the stretching sheet enhances on growing the Brownian motion parameter because the thermal boundary layer becomes thinner. Figure 13 presents the concentration profile boost for increasing the thermophoretic effect because the more nanoparticles pass away from the hot surface [30]. The concentration profile enhances correspond the chemical react impact shown in Figure 14.

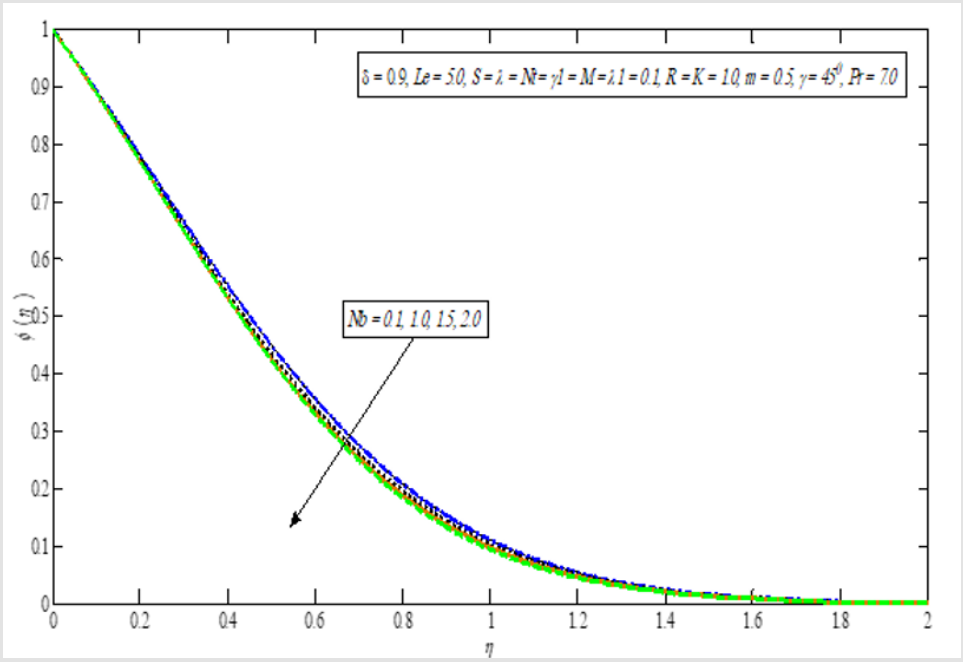

Figure 12: Concentration profile against Nb.

DOI: 10.26717/BJSTR.2023.48.007646

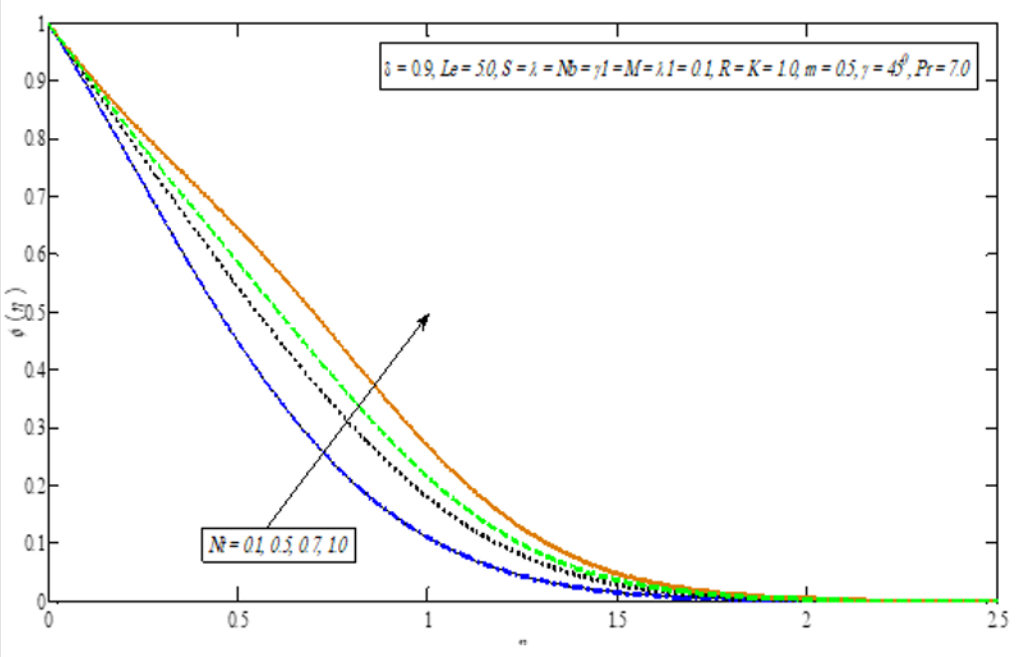

Figure 13: Concentration profile against Nt.

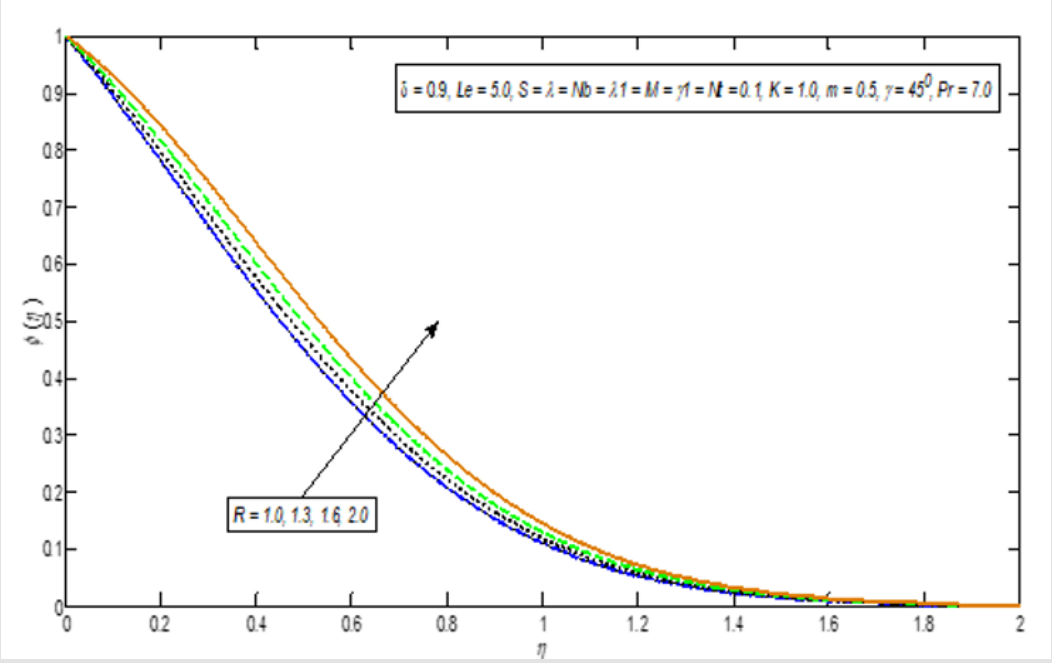

Figure 14: Concentration profile against R.

Conclusion

This problem has explored the micropolar nanofluid fluid flow over a nonlinear inclined stretching sheet by incorporating the chemical and heat generation or absorption impacts along with convective boundaries. The main findings of our current study are the following.

- The velocity field reduces correspond the higher values of the nonlinear stretching parameter.
- The heat transfer coefficient boost for bigger values of Biot number.
- The boundary layer becomes thicker on improving the Biot number.
- The nonlinear stretching parameter enhances the boundary layer thickness.
- The heat generation improves the velocity of the liquid.
- The growing values of chemical reaction improve the concentration outline.
- The concentration profile upturn against bigger values of the Biot number.

References

1. Choi SU, Eastman JA (1995) Enhancing thermal conductivity of fluids with nanoparticles. Argonne National Lab., IL (United States), p. 1-8.
2. Khan A, Khan D, Khan I, Ali F, ul Karim F, et al. (2018) MHD flow of Sodium Alginate-based Casson type nanofluid passing through a porous medium with Newtonian heating. Scientific reports 8(1): 8645.
3. Suriyakumar P, Devi SP A (2015) Effects of Suction and Internal Heat Generation on Hydromagnetic Mixed Convective Nanofluid Flow over an Inclined Stretching Plate 2(3): 51-58.
4. Khan M, Shahid A, Malik MY, Salahuddin T (2018) Thermal and concentration diffusion in Jeffery nanofluid flow over an inclined stretching sheet: A generalized Fourier's and Fick's perspective. Journal of Molecular Liquids 251: 7-14.
5. Thumma T, Beg OA, Kadir A (2017) Numerical study of heat source/sink effects on dissipative magnetic nanofluid flow from a non-linear inclined stretching/shrinking sheet. Journal of Molecular Liquids 232: 159-173.
6. Rashad A (2017) Unsteady nanofluid flow over an inclined stretching surface with convective boundary condition and anisotropic slip impact. International Journal of Heat and Technology 35(1): 82-90.
7. Govindarajan A (2018) Radiative fluid flow of a nanofluid over an inclined plate with non-uniform surface temperature. In Journal of Physics: Conference Series 1000(1): 12173.
8. Hatami M, Jing D, Yousif MA (2018) Three-dimensional analysis of condensation nanofluid film on an inclined rotating disk by efficient analytical methods. Arab Journal of Basic and Applied Sciences 25(1): 28-37.
9. Cimpean DS, Pop I (2012) Fully developed mixed convection flow of a nanofluid through an inclined channel filled with a porous medium. International journal of heat and mass transfer 55(4): 907-914.
10. Mjankwi MA, Masanja VG, Mureithi EW, James MN O (2019) Unsteady MHD Flow of Nanofluid with Variable Properties over a Stretching Sheet in the Presence of Thermal Radiation and Chemical Reaction. International Journal of Mathematics and Mathematical Sciences 31(4): 804-812.
11. Bohra S (2017) Heat and mass transfer over a three-dimensional inclined non-linear stretching sheet with convective boundary conditions. Indian Journal of Pure & Applied Physics 55(12): 847-856.
12. Bhuvaneswari M, Sivasankaran S, Ferdows M (2009) Lie group analysis of natural convection heat and mass transfer in an inclined surface with chemical reaction. Nonlinear Analysis: Hybrid Systems 3(4): 536-542.
13. Shit GC, Majee S (2014) Hydromagnetic Flow over an Inclined Non-Linear Stretching Sheet with Variable Viscosity in the Presence of Thermal Radiation and Chemical Reaction. Journal of Applied Fluid Mechanics 7(2): 239-247.
14. Sandeep N, Kumar MS (2016) Heat and Mass Transfer in Nanofluid Flow over an Inclined Stretching Sheet with Volume Fraction of Dust and Nanoparticles. Journal of Applied Fluid Mechanics 9(5): 2205-2215.
15. Reddy PB A (2016) Magnetohydrodynamic flow of a Casson fluid over an exponentially inclined permeable stretching surface with thermal radiation and chemical reaction. Ain Shams Engineering Journal 7(2): 593-602.
16. Rafique K, Anwar MI, Misiran M, Khan I, Seikh A H, et al. (2019) Brownian motion and thermophoretic diffusion effects on micropolar type nanofluid flow with Soret and Dufour impacts over an inclined sheet: Keller-box simulations. Energies 12(21): 4191.
17. Mjankwi MA, Masanja VG, Mureithi EW, James MN O (2019) Unsteady MHD Flow of Nanofluid with Variable Properties over a Stretching Sheet in the Presence of Thermal Radiation and Chemical Reaction. International Journal of Mathematics and Mathematical Sciences 2019(2): 1-14.
18. Rafique K, Anwar MI, Misiran M (2019) Keller-box Study on Casson Nano Fluid Flow over a Slanted Permeable Surface with Chemical Reaction 14(4): 1-17.
19. Alotaibi H, Rafique K (2021) Numerical Analysis of Micro-Rotation Effect on Nanofluid Flow for Vertical Riga Plate. Crystals 11(11): 1315.
20. Mitra A (2018) Computational Modelling of Boundary-Layer Flow of a Nano fluid Over a Convective Heated Inclined Plate. Journal of mechanics of continua and mathematical sciences 13(2): 88-94.
21. Eringen AC (1964) Simple microfluids. International Journal of Engineering Science 2(2): 205-217.
22. Rafique K, Anwar M I, Misiran M, Khan I, Seikh AH, et al. (2019) Numerical analysis with Keller-box scheme for stagnation point effect on flow of micropolar nanofluid over an inclined surface. Symmetry 11(11): 1379.
23. Rafique K, Anwar MI, Misiran M, Khan I, Seikh A H, et al. (2019) Keller-box simulation for the buongiorno mathematical model of micropolar nanofluid flow over a nonlinear inclined surface. Processes 7(12): 926.
24. Abbas N, Rehman KU, Shatanawi W, Al-Eid AA (2022) Theoretical study of non-Newtonian micropolar nanofluid flow over an exponentially stretching surface with free stream velocity. Advances in Mechanical Engineering 14(7): 16878132221107790.
25. Rafique K, Alotaibi H, Ibrar N, Khan I (2022) Stratified Flow of Micropolar Nanofluid over Riga Plate: Numerical Analysis. Energies 15(1): 316.
26. Srinivasacharya D, Bindu KH (2016) Entropy generation in a micropolar fluid flow through an inclined channel. Alexandria Engineering Journal 55(2): 973-982.
27. Hazbavi A, Sharhani S (2017) Micropolar Fluid Flow Between Two Inclined Parallel Plates. In ASME 2017 International Mechanical Engineering Congress and Exposition 8: V008T10A085.
28. Khan W A, Pop I (2010) Boundary-layer flow of a nanofluid past a stretching sheet. International journal of heat and mass transfer 53(11-12): 2477-2483.
29. Rafique K, Anwar MI, Misiran M, Khan I, Baleanu D, et al. (2020) Hydromagnetic flow of micropolar nanofluid. Symmetry. 12(2): 251.
30. Hayat T, Khan MI, Waqas M, Alsaedi A (2017) Newtonian heating effect in nanofluid flow by a permeable cylinder. Results in Physics 7: 256-262.

ISSN: 2574-1241

DOI: 10.26717/BJSTR.2023.48.007646

Khuram Rafique. Biomed J Sci & Tech Res